PHYSICAL REVIEW B **83**, 121410(R) (2011)

Improved lattice constants, surface energies, and CO desorption energies from a semilocal density functional

Jianwei Sun,[1] Martijn Marsman,[2] Adrienn Ruzsinszky,[1] Georg Kresse,[2] and John P. Perdew[1]
[1]*Department of Physics and Quantum Theory Group, Tulane University, New Orleans, Louisiana 70118, USA*
[2]*Faculty of Physics and Center for Computational Materials Science, University of Vienna, Sensengasse 8/12, A-1090 Wien, Austria*
(Received 21 February 2011; published 28 March 2011)

Using the revised Tao-Perdew-Staroverov-Scuseria (revTPSS) metageneralized gradient approximation, a computationally efficient semilocal functional, we studied the desorption energies of the molecule CO on the (111) surfaces of transition metals as well as the surface energies and lattice constants of the underlying transition metals. Due to its ability to distinguish single-orbital regions from regions of high orbital overlap, revTPSS improves all three properties over the Perdew-Burke-Ernzerhof (PBE) generalized gradient approximation. No generalized gradient approximation matches this performance, which has been regarded as unreachable by semilocal approximations.

DOI: 10.1103/PhysRevB.83.121410 PACS number(s): 68.43.Bc, 82.65.+r

The adsorption of carbon monoxide on transition metal surfaces has been the subject of many studies. Together with hydrogen adsorption and dissociation, it is often regarded as a classical benchmark for experimental and theoretical surface science techniques. Among theoretical techniques, the Kohn-Sham density functional theory (KS-DFT),[1] which describes surfaces and adsorbate structures on the atomic scale, is one of the most popular. The accuracy of KS-DFT is dependent on the choice of exchange-correlation functional, the only approximated part of the method. In a now-classic paper, Feibelman *et al.*[2] studied the CO molecule adsorbed on the Pt(111) surface and found that the Perdew-Wang (PW)91 and Perdew-Burke-Ernzerhof (PBE) generalized gradient approximation (GGA) functionals fail qualitatively to predict the site preference of CO adsorption on the Pt(111) surface, standing the CO molecule carbon-down on the fcc hollow site rather than on the top site observed experimentally. Since then, almost all five rungs of the Jacob's ladder of density functional approximations[3] have been tested for this puzzle,[4–8] except for the metageneralized gradient approximation (MGGA) rung.

Although the site-preference problem is a significant issue, there is a more troublesome dilemma[5]: Semilocal density functionals have a general tendency to underestimate surface energies and to overestimate chemisorption energies. Modifying the semilocal functional can apparently correct one of these properties but not both, implying that reliable surface reconstructions could not be predicted together with accurate desorption energies from a computationally efficient semilocal functional. However, this dilemma has only been demonstrated for the semilocal functionals at the local density approximation (LDA) and GGA levels. It can be avoided by climbing to the MGGA level, as suggested in this study by using the nonempirical revTPSS MGGA.[9]

The *ab initio* calculations presented here were carried out using the VASP code with projector augmented wave[10] (PAW) potentials in the implementation of Kresse and Joubert.[11] Adequate kinetic energy density was provided for MGGA's, and a plane-wave cutoff energy of 500 eV was used. As trends are the main focus of this study, all metals were considered in the fcc structure, although Ru crystallizes in the hcp structure. Adsorption at the top and fcc hollow sites was considered for Cu, Pd, Ag, and Pt, whereas for Ru and Rh the top and hcp hollow sites were considered. In each case, the hollow site considered was the one preferred by revTPSS. The supercell for the system consists of periodic six-layer slabs with $c(2 \times 4)$ in-plane periodicity, a CO molecule adsorbed on one side of the slab, and a vacuum space of about 10 Å. The CO molecule is relaxed along with two adjacent metal layers for each functional implemented self-consistently, including the revTPSS MGGA.[12] For Brillouin-zone integrations, symmetry-reduced Γ-centered $8 \times 8 \times 1$ grids were used. For the sake of clearer discussion and figures, we show the desorption energy $E_{\rm des} = E(\rm CO) + E(\rm surface) - E(\rm CO + surface) = -E_{\rm ads}$, where $E_{\rm ads}$ is the adsorption energy.

Figure 1(a) plots the calculated surface energies versus the calculated atop desorption energies for CO on Pt(111) and Rh(111) surfaces. It shows that, with increasing surface energy, the desorption energy increases as well, the same dilemma observed by Schimka *et al.*[5] for semilocal functionals at the LDA and GGA levels. Results from the LDA,[1,13] and from the GGA's PBE,[14] the PBE for solids[15] (PBEsol) with a diminished gradient dependence,[16] and the revised PBE (rPBE) for desorption energies[17] lie roughly on straight lines. However, the semilocal revTPSS MGGA lies off the straight lines and closer to the experimental values, yielding excellent surface energies and fairly good desorption energies. Obviously, the revTPSS MGGA has already stepped out of the dilemma that was believed to hold for all semilocal functionals.

Semilocal approximations of the form

$$E_{\rm xc}[n_\uparrow, n_\downarrow] = \int d^3r\, n e_{\rm xc}(n_\uparrow, n_\downarrow, \nabla n_\uparrow, \nabla n_\downarrow, \tau_\uparrow, \tau_\downarrow) \quad (1)$$

require only a single integral over real space and so are dramatically less expensive than nonlocal functionals, e.g., the PBE0 (Refs. 18 and 19) and Heyd-Scuseria-Ernzerhof (HSE)03 (Ref. 20) hybrid functionals and the random phase approximation (RPA) in a density functional context,[21] which involve a double integral over real space. In Eq. (1), $n = n_\uparrow + n_\downarrow$ is the electron density and $\tau_\sigma = \sum_i |\nabla \psi_{i\sigma}|^2/2$ is the positive kinetic energy density; all equations are in atomic units. Since all the calculations considered here are spin unpolarized, the spin will be suppressed in the following

discussions. The LDA (Refs. 1 and 13) uses only the ingredient n and is exact for a uniform electron gas. LDA is a reasonable functional for properties of extended systems (e.g., lattice constant and surface energy), but unacceptable for properties (e.g., atomization energy and desorption energy) of confined systems where the electron densities are more inhomogeneous and further away from the uniform electron gas.

GGA's (Refs. 14, 15, and 17) add the ingredient ∇n and improve over LDA the properties of confined systems. The enhancement factors of different exchange functionals, defined as $F_x = e_x/e_x^{\text{unif}}$, where $e_x^{\text{unif}} = -3(3\pi^2 n)^{1/3}/4\pi$ is the exchange energy per electron of a uniform electron gas of density n, are shown in Fig. 1(b) as a function of the reduced density gradient $s = |\nabla n|/[2(3\pi^2 n)^{1/3} n]$, a measure of inhomogeneity. The exchange enhancement factor F_x is 1 in LDA and monotonically increases with s in GGA's. The larger the enhancement factor of a GGA, the more preference the GGA has toward inhomogeneity. To cure the unacceptable LDA overestimation of desorption energies, the enhancement factor must be increased. Then, the inability of GGA to distinguish between the same reduced density gradient in different regions inevitably results in the reduction of surface energies, which leads to the straight lines in Fig. 1(a). Therefore, in the LDA and GGA world, the best that a functional can do is to be at the projection of the experimental point on the line.

However, by adding the ingredient τ, MGGA's, e.g., the revTPSS in Fig. 1(b), can distinguish single-orbital regions ($\alpha = 0$) from orbital-overlap regions ($\alpha \gtrsim 1$),[22] and thus have the potential to describe well both confined and extended systems. Here, $\alpha = (\tau - \tau^W)/\tau^{\text{unif}}$, where $\tau^W = |\nabla n|^2/8n$ is the von Weizsäcker kinetic energy density and $\tau^{\text{unif}} = n(3/10)(3\pi^2 n)^{2/3}$ is the orbital kinetic energy density of the uniform electron gas. For a slowly varying density ($\tau \approx \tau^{\text{unif}}$ and $\tau^W \ll \tau^{\text{unif}}$), α approaches 1, where, as does PBEsol, revTPSS restores the second-order gradient expansion for exchange over a wide range of densities. However, for a one- or two-electron density ($\tau = \tau^W$), where $\alpha = 0$, revTPSS has a larger enhancement factor than for $\alpha = 1$. Thus, revTPSS shows less preference than does PBEsol for the overlapping of electron orbitals usually involved in molecular formation and certainly involved in the adsorption of CO, as explained below. Indeed, Fig. 1(a) shows that revTPSS yields surface energies slightly better than its underlying PBEsol GGA and at the same time reduces the overestimation of desorption energies from the PBEsol to the PBE level or better.

The revTPSS MGGA also manifests its ability to distinguish single-orbital regions from orbital-overlapped regions in the density of states (DOS) of CO adsorbed on Pt(111). A common model to describe CO adsorption[5,25] invokes resonant interactions of the two CO frontier orbitals, the occupied 5σ (which, in the isolated molecule, represents a loosely bound lone pair on the carbon atom, directed away from the oxygen atom) and the unoccupied $2\pi^*$, with those metal orbitals that lie close to them in energy. Bonding and antibonding 5σ-metal orbitals develop in a broad band, the center of which is shifted below the occupied 1π CO orbitals. The broadened antibonding orbitals are partly shifted above the Fermi level, causing a net bonding interaction with electron donation to the metal. Similarly, bonding $2\pi^*$-metal orbitals become partly populated, with back donation. Both processes strengthen the adsorption. Simple symmetry tells us that the highly directional 5σ-metal interaction is particularly strong for atop adsorption, while the $2\pi^*$ interaction dominates for hollow-site adsorption.[26] 1π denotes the lowest degenerate pair of bonding π orbitals, and $2\pi^*$ the lowest degenerate pair of antibonding π orbitals.

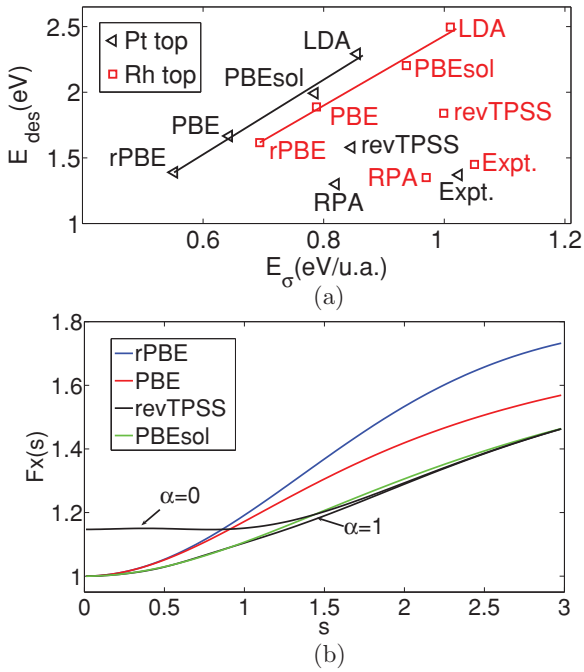

FIG. 1. (Color) (a) Atop CO desorption energy vs surface energies for Pt(111) and Rh(111). RPA values from Ref. 5, experimental surface energies from liquid-metal data (Refs. 23 and 24), and experimental CO desorption energies from Ref. 7. Surface energies are per surface-plane atom. (b) Exchange enhancement factors of semilocal functionals as functions of the reduced density gradient s. $\alpha = 0$: single-orbital region, and $\alpha = 1$: slowly varying density for $s \ll 1$ (Ref. 9).

Figure 2 shows the DOS of different semilocal functionals projected onto the nearest four surface Pt atoms and onto the CO molecule, adsorbed atop a Pt atom on Pt(111). At the GGA level, the d-band width in the weakly overlapped range between 0 (the Fermi level) and -6 eV decreases and the d-band center moves up toward the Fermi energy from PBEsol to PBE and then to rPBE, in order of increasing exchange enhancement factor. The DOS projected onto the CO molecules shown in Fig. 2(b) is less sensitive to the choice of GGA. This results in the decrease of the desorption energies from PBEsol to PBE then to rPBE, since a narrower d band implies a weaker overlap with the 5σ and $2\pi^*$ orbitals. The revTPSS MGGA recovers the PBEsol to a large extent for a slowly varying density and thus delivers almost the identical d band and slightly better surface energy compared to PBEsol. However, revTPSS shifts down the 1π as well as 5σ and shifts up the $2\pi^*$ of the CO molecule compared to PBEsol, resulting in weaker net bonding between the two frontier orbitals of CO and the metal orbitals, thereby reducing the overestimation of the desorption energy.

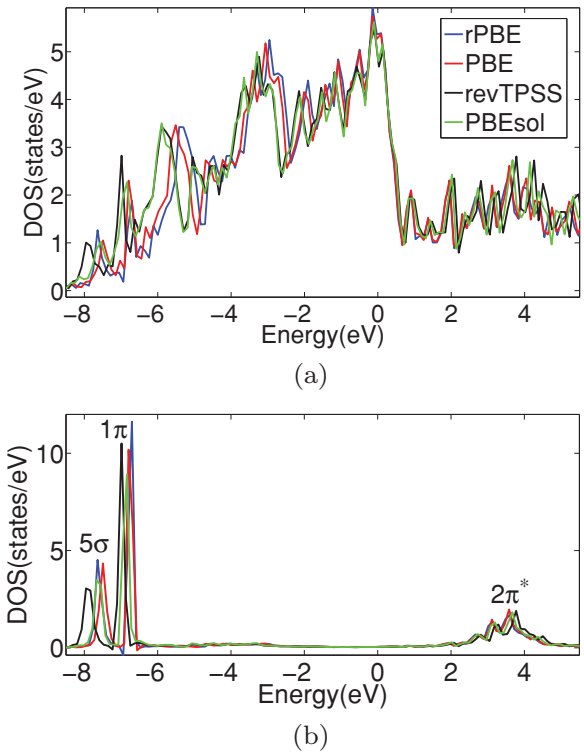

FIG. 2. (Color) Electronic DOS for CO atop adsorption on Pt(111) from semilocal density functionals. The upper panel shows the DOS on the surface Pt atoms (including part of the 5σ), and the bottom panel shows the DOS on the CO.

Figure 3 shows the desorption energies of CO on different transition metal (111) surfaces as well as the lattice constants and surface energies of the underlying transition metals. The minima of Figs. 3(b) and 3(c) at Cu and Ag reflect the weaker bonding in the noble metals. For the considered GGA functionals, the PBEsol lattice constants and surface energies (green lines) are best with relative errors in lattice constants less than 1% for each transition metal and with errors in surface energies less than 0.25 eV/u.a., while the rPBE desorption energies (blue lines) are the most accurate except for the Ag surface, where CO is incorrectly predicted to desorb spontaneously with error 0.3 eV. The PBEsol desorption energies are unacceptably high, while rPBE predicts too large lattice constants and too low surface energies. PBE turns out to be the most balanced GGA, delivering values for these three properties with errors between those of PBEsol and rPBE. Due to reasons already mentioned, the revTPSS MGGA delivers similar lattice constants and slightly better surface energies compared to PBEsol, and at the same time improves the desorption energies over PBEsol to the PBE level or better. This suggests that, for all the properties considered here, which are important to surface science, the revTPSS MGGA outperforms PBE, the most popular GGA. Ours is the first demonstration that MGGA's can give accurate surface energies for real materials, as for jellium.[9]

However, the revTPSS MGGA does not predict the correct adsorption sites for CO adsorbed on Cu, Rh, and Pt (111) surfaces, as shown in Fig. 3(c), putting CO on the high-

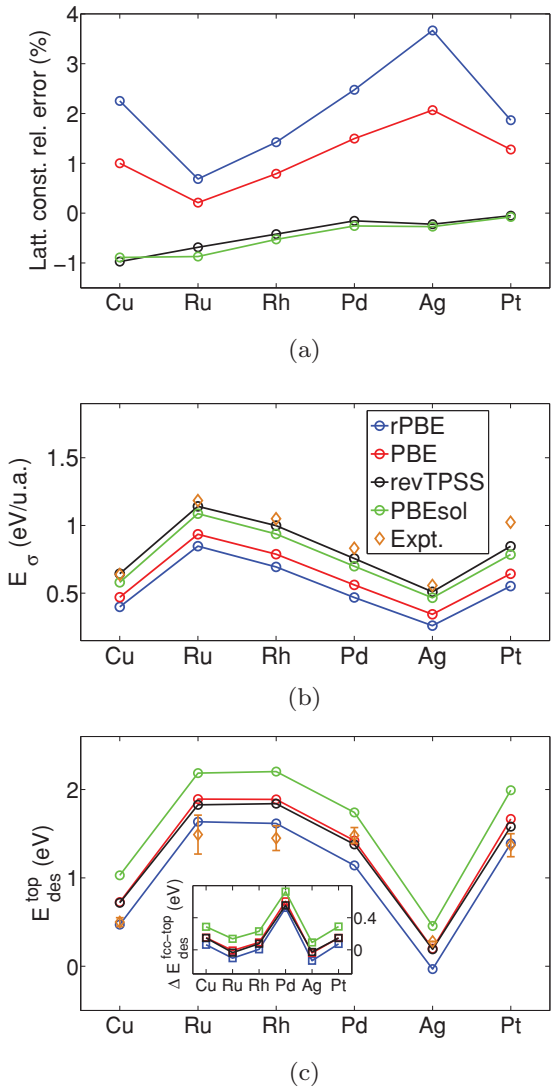

FIG. 3. (Color) (a) Lattice constants from semilocal density functionals. The experimental values for Cu, Rh, Pd, Ag, and Pt from Ref. 27 have been corrected by subtracting the zero-point anharmonic expansion (ZPAE) from the experimental zero-temperature values. The experimental lattice constant of Ru is taken from Ref. 28, which is calculated from the experimental hcp volume assuming an fcc structure. (b) Fcc(111) surface energies (E_σ) from semilocal density functionals. Experimental surface energies are deduced from liquid-metal data (Refs. 23 and 24). (c) Desorption energies for the atop site of CO on Cu, late $4d$ metals and Pt from semilocal density functionals. The energy difference $\Delta E_{\rm des}^{\rm fcc-top} = E_{\rm des}^{\rm fcc} - E_{\rm des}^{\rm top}$, indicating the site preference, is shown in the inset for each metal. Experimental data with error bars are from Ref. 7. The error bars correspond to the spread of the experimental results.

coordination hollow site rather than on the top site observed experimentally. The quantitative error is not large, but the qualitative error remains. There have been efforts to correct this error by using nonlocal functionals. Stroppa *et al.*[4] applied the hybrid GGA's PBE0 (Refs. 18 and 19) and HSE03 (Ref. 20) to this CO/Pt(111) puzzle and showed that climbing the ladder from GGA's to hybrid GGA's does not necessarily improve the desorption energies and site preference. The PBE0 and the

range-separated hybrid GGA HSE03 improve the predicted site preference over PBE, but still not enough to predict the right adsorption site. Furthermore, the desorption energies predicted by these two hybrid GGA's are even higher for both sites than those of PBE, and thus even further away from the experimental results. The Becke-3-Lee-Yang-Parr (B3LYP) hybrid GGA (Refs. 29–32) predicts the right adsorption site and accurate desorption energies,[8] but it fails to predict accurate lattice constants and surface energies, as does its underlying BLYP GGA.[33]

Schimka *et al.*[5] found that RPA,[21] a nonlocal functional on the highest rung of Jacob's ladder, delivered correct adsorption sites with accurate desorption energies as well as accurate surface energies and lattice constants for the underlying transition metals. The good performance of RPA might suggest that the CO/Pt(111) puzzle is nonlocality-related, although the nonlocality in this problem is not large. However, the computational load for RPA is dramatically heavier than for semilocal functionals. The revTPSS MGGA delivers overall very respectable performance at about 1% of the computational cost of RPA. This work confirms that revTPSS is the workhorse functional for condensed matter physics (or at least for surface science) that it promised to be.[9]

We thank Gábor I. Csonka for helpful discussions. This work was partially supported by the IMI Program of the National Science Foundation under Award No. DMR04-09848, and at Tulane by NSF under Grant No. DMR08-54769. Portions of this research were conducted with high performance computational resources provided by the Louisiana Optical Network Initiative [http://www.loni.org/]. G.K. and M.M. acknowledge support of the Austrian FWF within the SFB ViCoM (F41).

[1] W. Kohn and L. J. Sham, Phys. Rev. A **140**, 1133 (1965).
[2] P. J. Feibelman, B. Hammer, J. K. Norskov, F. Wagner, M. Scheffler, R. Stumpf, R. Watwe, and J. Dumesic, J. Phys. Chem. B **105**, 4018 (2001).
[3] J. P. Perdew and K. Schmidt, in *Density Functional Theory and Its Applications to Materials*, edited by V. E. van Doren, C. van Alsenoy, and P. Geerlings (American Institute of Physics, New York, 2001).
[4] A. Stroppa, K. Termentzidis, J. Paier, G. Kresse, and J. Hafner, Phys. Rev. B **76**, 195440 (2007).
[5] L. Schimka, J. Harl, A. Stroppa, A. Grueneis, M. Marsman, F. Mittendorfer, and G. Kresse, Nat. Mater. **9**, 741 (2010).
[6] M. Alaei, H. Akbarzadeh, H. Gholizadeh, and S. de Gironcoli, Phys. Rev. B **77**, 085414 (2008).
[7] F. Abild-Pedersen and M. P. Andersson, Surf. Sci. **601**, 1747 (2007).
[8] K. Doll, Surf. Sci. **573**, 464 (2004).
[9] J. P. Perdew, A. Ruzsinszky, G. I. Csonka, L. A. Constantin, and J. Sun, Phys. Rev. Lett. **103**, 026403 (2009).
[10] P. E. Blöchl, Phys. Rev. B **50**, 17953 (1994).
[11] G. Kresse and D. Joubert, Phys. Rev. B **59**, 1758 (1999).
[12] J. Sun, M. Marsman, G. I. Csonka, A. Ruzsinszky, P. Hao, Y.-S. Kim, G. Kresse, and J. P. Perdew (unpublished).
[13] J. P. Perdew and Y. Wang, Phys. Rev. B **45**, 13244 (1992).
[14] J. P. Perdew, K. Burke, and M. Ernzerhof, Phys. Rev. Lett. **77**, 3865 (1996).
[15] J. P. Perdew, A. Ruzsinszky, G. I. Csonka, O. A. Vydrov, G. E. Scuseria, L. A. Constantin, X. Zhou, and K. Burke, Phys. Rev. Lett. **100**, 136406 (2008).
[16] G. I. Csonka, O. A. Vydrov, G. E. Scuseria, A. Ruzsinszky, and J. P. Perdew, J. Chem. Phys. **126**, 244107 (2007).
[17] B. Hammer, L. B. Hansen, and J. K. Nørskov, Phys. Rev. B **59**, 7413 (1999).
[18] M. Ernzerhof and G. E. Scuseria, J. Chem. Phys. **110**, 5029 (1999).
[19] C. Adamo and V. Barone, J. Chem. Phys. **110**, 6158 (1999).
[20] J. Heyd, G. E. Scuseria, and M. Ernzerhof, J. Chem. Phys. **118**, 8207 (2003).
[21] D. C. Langreth and J. P. Perdew, Phys. Rev. B **21**, 5469 (1980).
[22] J. Tao, J. P. Perdew, V. N. Staroverov, and G. E. Scuseria, Phys. Rev. Lett. **91**, 146401 (2003).
[23] W. R. Tyson and W. A. Miller, Surf. Sci. **62**, 267 (1977).
[24] L. Vitos, A. V. Ruban, H. L. Skriver, and J. Kollar, Surf. Sci. **411**, 186 (1998).
[25] G. J. Blyholder, J. Phys. Chem. **68**, 2772 (1964).
[26] R. A. van Santen, *Molecular Heterogeneous Catalysis: A Conceptual and Computational Approach* (Wiley, New York, 2006).
[27] P. Haas, F. Tran, and P. Blaha, Phys. Rev. B **79**, 085104 (2009).
[28] A. Stroppa and G. Kresse, New J. Phys. **10**, 063020 (2008).
[29] A. D. Becke, J. Chem. Phys. **98**, 5648 (1993).
[30] P. J. Stephens, F. J. Devlin, C. F. Chabalowski, and M. J. Frisch, J. Phys. Chem. **98**, 11623 (1994).
[31] A. D. Becke, Phys. Rev. A **38**, 3098 (1988).
[32] C. Lee, W. Yang, and R. G. Parr, Phys. Rev. B **37**, 785 (1988).
[33] S. Kurth, J. P. Perdew, and P. Blaha, Int. J. Quantum Chem. **75**, 889 (1999).